Revealing Complex Traits with Small Molecules and Naturally Recombinant Yeast Strains

Ethan O. Perlstein,[1] Douglas M. Ruderfer,[3]
Gopal Ramachandran,[4] Stephen J. Haggarty,[4]
Leonid Kruglyak,[3] and Stuart L. Schreiber[1,2,4,*]
[1] Department of Molecular and Cellular Biology
[2] Department of Chemistry and Chemical Biology
Howard Hughes Medical Institute
Harvard University
Cambridge, Massachusetts 02138
[3] Lewis-Sigler Institute for Integrative Genomics and
Department of Ecology and Evolutionary Biology
Carl Icahn Laboratory
Princeton University
Princeton, New Jersey 08544
[4] Broad Institute of Harvard and MIT
7 Cambridge Center
Cambridge, Massachusetts 02142

Summary

Here we demonstrate that natural variants of the yeast *Saccharomyces cerevisiae* are a model system for the systematic study of complex traits, specifically the response to small molecules. As a complement to artificial knockout collections of *S. cerevisiae* widely used to study individual gene function, we used 314- and 1932-member libraries of mutant strains generated by meiotic recombination to study the cumulative, quantitative effects of natural mutations on phenotypes induced by 23 small-molecule perturbagens (SMPs). This approach reveals synthetic lethality between SMPs, and genetic mapping studies confirm the involvement of multiple quantitative trait loci in the response to two SMPs that affect respiratory processes. The systematic combination of natural variants of yeast and small molecules that modulate evolutionarily conserved cellular processes can enable a better understanding of the general features of complex traits.

Introduction

The extensive use of artificial single-gene knockout collections of the budding yeast *Saccharomyces cerevisiae* [1] over the last decade has substantially increased our knowledge of conserved eukaryotic cellular processes. Although the use of gene-deletion collections simplifies the tedious process of matching a mutation to an observed phenotype, it only permits the study of the effects of deleting single genes or pairs of genes [2], as opposed to combinations of loss- and gain-of-function alleles of multiple genes. Most genetic traits are complex (i.e., are encoded by allelic variants of at least two different genes whose individual contributions have graded effects, varying from small to large) [3–5]. In this study, we build on the base of gene-deletion collections by using natural genetic variation, as opposed to

artificial mutations, in yeast as a means to study complex traits—specifically, the response of cells (e.g., resistance or sensitivity) to small molecules [6, 7]. The use of small molecules to reveal complex traits was first suggested by studies of metabolism in *Neurospora* over 60 years ago [8]. More recently, *S. cerevisiae* has been exploited as a means to study global mRNA levels as a complex trait, where *cis*- and *trans*-acting loci that heritably modulated the level of each transcript were identified [9, 10]. Another study has described quantitative enological traits (e.g., ethanol tolerance) in winemaking, industrial strains of yeast [11], among others [12]. Now that the genome sequences of three variants of *S. cerevisiae*—a clinical isolate, an agricultural isolate, and a common laboratory strain—are in hand, it will be possible to identify tens of thousands of genetically encoded polymorphisms. However, whether these polymorphisms are functionally neutral or functionally active is unknown. Here we show that small molecules can be used systematically in yeast to link natural genetic variation to physiological phenotypes.

Results and Discussion

We identified 23 small-molecule perturbagens (SMPs) (see Table S1 in the Supplemental Data available online) that differentially inhibit the growth of one or more of three diploid yeast strains that were the focus of an unrelated study to dissect the architecture of a quantitative trait in yeast [13]: S1029, YAG040, and XHS123; a commonly used laboratory homozygous diploid, a clinical isolate homozygous diploid derived over 20 years ago from the lungs of an AIDS patient in San Francisco, and the heterozygous diploid formed by crossing the laboratory strain and the clinical isolate, respectively. The genome sequence of a strain isogenic to YAG040 was recently sequenced [14], setting the stage for the systematic characterization of polymorphisms between it and the already-sequenced lab strain. XHS123 and YAG040 were constructed with artificial dominant drug resistance markers kanMX and hphMX, respectively, both of which serve as standards of Mendelian, single-gene traits.

The 23 SMPs are chemically diverse and differ in their reported mechanisms of action, with the exception of functional analogs, which will be further discussed below. They are evenly divided between natural products and synthetic products, and seven are Food and Drug Administration (FDA)-approved drugs. Many have been studied almost exclusively in the context of mammalian cells; for example, the central nervous system-active compounds flunarizine and pimozide. These SMPs are shown here to inhibit potently the growth of yeast in a genotype-dependent and heritable manner.

We generated resistance/sensitivity profiles of two libraries (differing only in size) comprising 314 and 1932 random XHS123 meiotic segregants in order to characterize the complexity of resistance or sensitivity to each SMP at or near its IC_{50} concentration (Figure S1). Generally, growth inhibition by a small molecule segregates
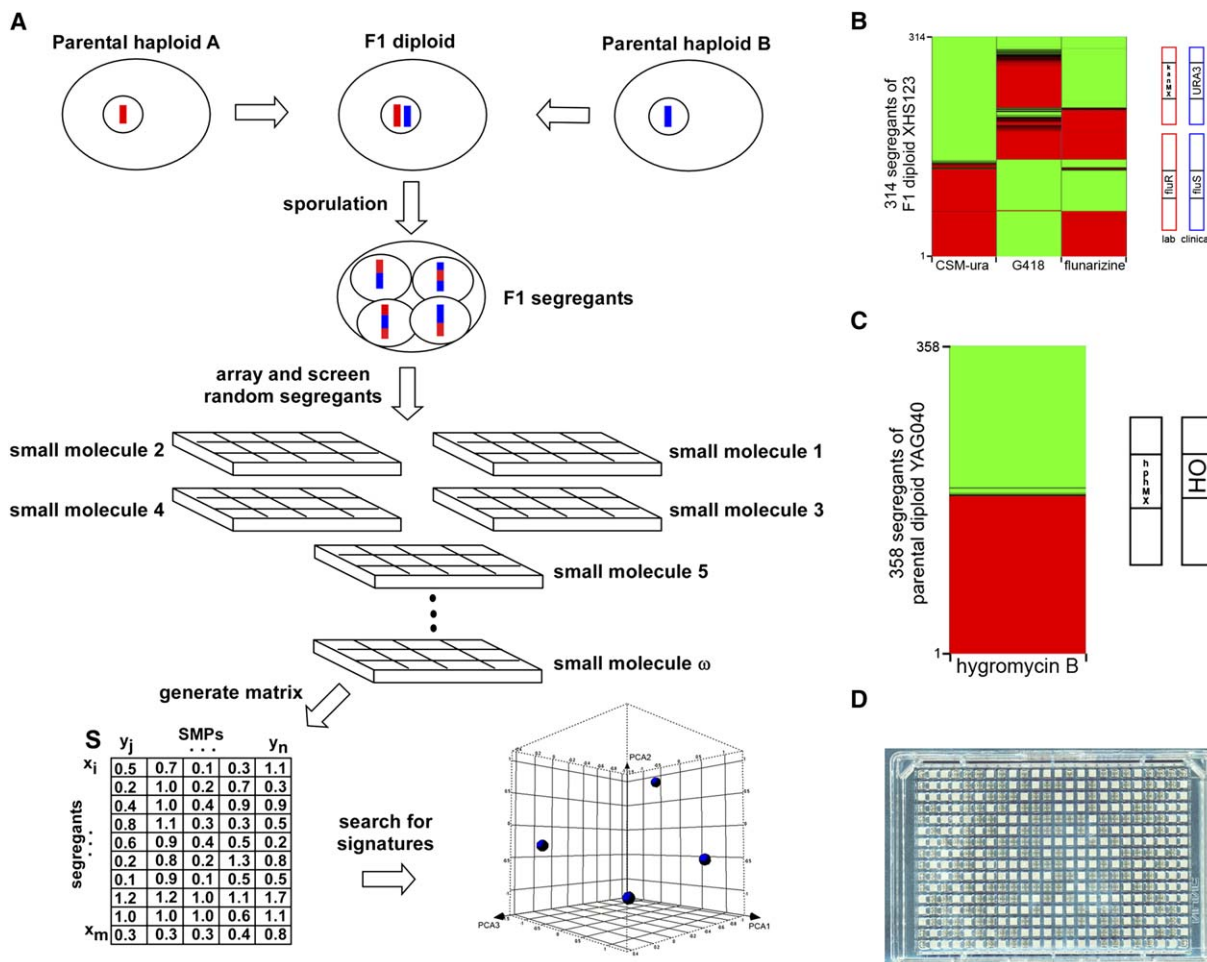
*Correspondence: stuart_schreiber@harvard.edu

Figure 1. Overview of the Generation and Pertubational Chemical Profiling of Random Meiotic Segregants of XHS123

(A) Two haploid yeast strains—in this study, derivatives of S1029 and YAG040—are mated in order to generate an F1 heterozygous diploid, which was subsequently sporulated, yielding F1 segregants. Averaged, quantitative growth measurements of random segregants in multiple conditions were arranged into a matrix and computationally analyzed.

(B) Segregation of two unlinked Mendelian traits illustrated by a heat map (red indicates saturating growth, or resistance; green indicates no growth, or sensitivity) of clustered OD_{600} measurements of 314 XHS123 segregants grown in complete synthetic media lacking uracil (CSM-URA); rich media containing 200 μg/ml G418; rich media containing 50 μg/ml flunarizine (SMP9). Half of XHS123 segregants were resistant to G418, conferred by the kanMX cassette, but unable to grow without supplemental uracil, or vice versa. One-quarter of segregants were resistant to both G418 and flunarizine; one-quarter were resistant to G418 but sensitive to flunarizine; one-quarter were sensitive to G418 but resistant to flunarizine; one-quarter were sensitive to both G418 and flunarizine.

(C) Segregation of a single Mendelian trait illustrated by a heatmap of clustered OD_{600} measurements of 358 YAG040 segregants grown in rich media containing 300 μg/ml of the antibiotic hygromycin B. Half of YAG040 segregants were resistant to hygromycin B, conferred by hphMX cassette (i.e., were haploid); half were sensitive; that is, they inherited the wild-type copy of the HO gene, which enables self-diploidization (i.e., were diploid).

(D) Digital optical scan of clear-bottom, 384-well plate containing 366 random YAG040 segregants. Visual inspection of the number of wells containing growth (192) versus those not containing growth (176) clearly indicates Mendelian segregation of hygromycin B resistance (192 resistant/368 sensitive [52%]).

either in a Mendelian (i.e., monogenic) or a complex (i.e., polygenic) fashion. As expected, the aforementioned dominant drug resistance markers segregated as Mendelian traits (Figures 1B and 1C). We next determined whether growth inhibition by each SMP segregates in a Mendelian or a complex fashion. As compared to the control Mendelian trait, resistance to G418, which is conferred by the kanMX cassette, growth inhibition by all SMPs was found to be complex to varying degrees, with the exception being flunarizine (SMP9) (Figure 2B), a calcium ion (Ca^{2+}) channel blocker [15], which appeared to be a Mendelian trait at 48 hr postinoculation.

Interestingly, however, at 72 hr, one-quarter of segregants remained sensitive, while three-quarters became resistant to flunarizine, suggesting a more complex genetic underpinning to resistance: two sensitizing alleles—one fast-acting (48 hr), the other slow-acting (72 hr) (Figure 2B). In addition to being complex, growth inhibition by the majority of SMPs also has a kinetic component. The response to rapamycin (SMP45) exemplifies the variegated temporal and quantitative nature of complex growth inhibition by a small molecule (Figure 2C). We also observed both Mendelian and complex growth inhibition that was not induced by an SMP, but
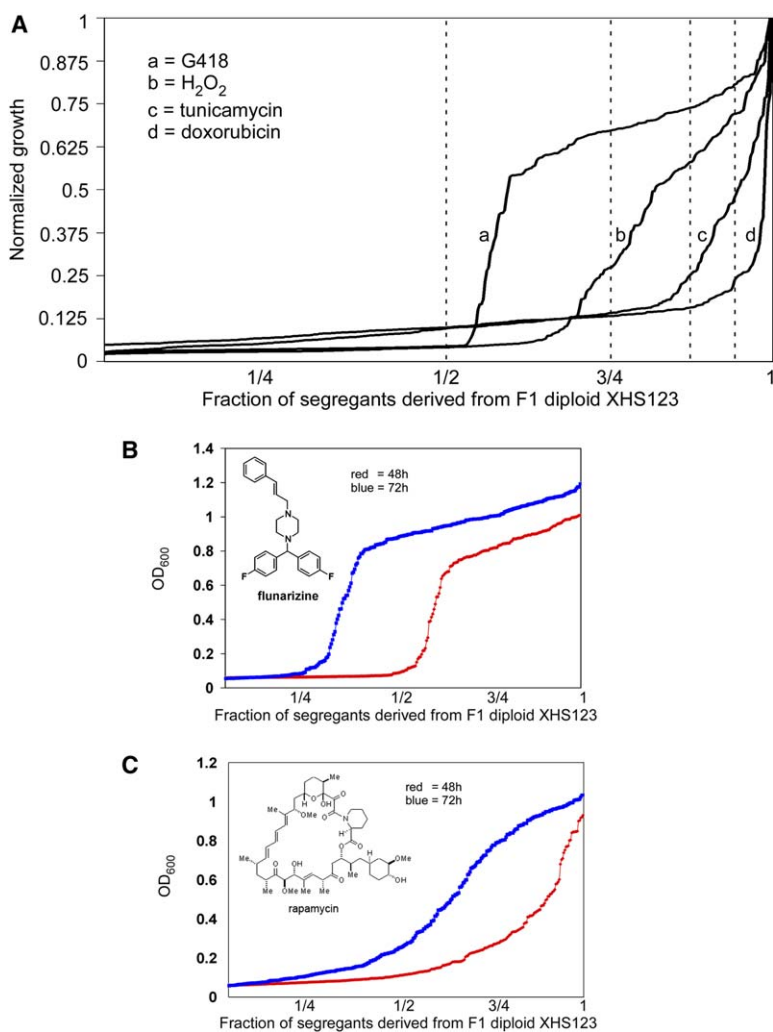
Figure 2. Rank-Ordered Distributions of XHS123 Segregants Demonstrate that Growth Inhibition by Small Molecules Is Polygenic, Kinetic, and Quantitative

(A) A total of 375 XHS123 *MAT*a segregants from the 1932 member library are plotted on a 1D graph, where the x axis denotes the fraction of the segregant population and the y axis denotes normalized OD_{600} values: a = rich media containing 200 μg/ml G418; b = 0.015% H_2O_2; c = 200 ng/ml tunicamycin (SMP13); d = 25 μg/ml doxorubicin (SMP7). Dashed vertical lines appear at 1/2, 3/4, 7/8, and 15/16 marks.
(B) Rank-ordered distribution of 314 XHS123 segregants in 50 μg/ml flunarizine (SMP9). The red curve corresponds to measurements taken at 48 hr; the blue curve corresponds to measurements taken at 72 hr. The chemical structure of flunarizine appears in upper left corner of the graph.
(C) Rank-ordered distribution of 314 XHS123 segregants in 500 ng/ml rapamycin (SMP45). The red curve corresponds to measurements taken at 48 hr; the blue curve corresponds to measurements taken at 72 hr. The chemical structure of rapamycin appears in the upper left corner of the graph.

rather by constituents of so-called stress media: rich media containing 0.9 M sodium chloride (NaCl); synthetic wine must (SWM), which combines osmotic and pH shock; and growth on media containing maltose as the sole carbon source (Figures S2A–S2C). Any nongenetic variables (e.g., experimental noise or epigenetic effects) play a minor role in our method, as revealed by strong agreement between experimental replicates. Disagreement between replicates is greatest at mid-log phase OD_{600} values, as expected, as they would be most sensitive to experimental variation (e.g., inoculum size), while low and high OD_{600} values, corresponding to hypersensitivity and resistance, are highly reproducible (Figure S3).

We estimated the complexity of growth inhibition by each SMP: the approximate number of genetic determinants that underlie resistance (or sensitivity). The ranked-order distributions of 375 *MAT*a XHS123 segregants in the presence of G418, H_2O_2, tunicamycin (SMP13), and doxorubicin (SMP7) illustrate a series of four complex traits underlain by increasing numbers of genetic determinants (Figure 2A). The 375 *MAT*a XHS123 segregants comprise a portion of the 1932 member library, and were chosen to eliminate any possible confounding effects of ploidy. If we assume that

the fraction of the resistant segregants approximates $\frac{1}{2}^n$, where n equals the number of underlying genetic determinants at a given kinetic snapshot and concentration, then a single gene underlies resistance to G418, two underlie resistance to H_2O_2, three underlie resistance to tunicamycin, and four underlie resistance to doxorubicin. The number of genetic determinants that underlie resistance fell within this range (1–4) for all 23 SMPs (Figure S4), although the quantitative nature of these traits makes it difficult to predict the exact number of determinants. Although "off-target" effects could confound the true breadth of this range, many of the SMPs are natural products (e.g., rapamycin) that display known fine specificity for their molecular targets. Indeed, our results are consistent with previous studies, which found that multiple heterozygous whole-gene deletion strains are haploinsufficient in response to perturbation by a small molecule [16].

After establishing that sensitivity or resistance to a small molecule can be a complex trait, we addressed whether the same genetic determinants were responsible for resistance to all SMPs (i.e., a nonspecific multidrug efflux effect), or whether a unique set of genes selectively confers resistance to each SMP (i.e., random segregation and independent assortment of distinct
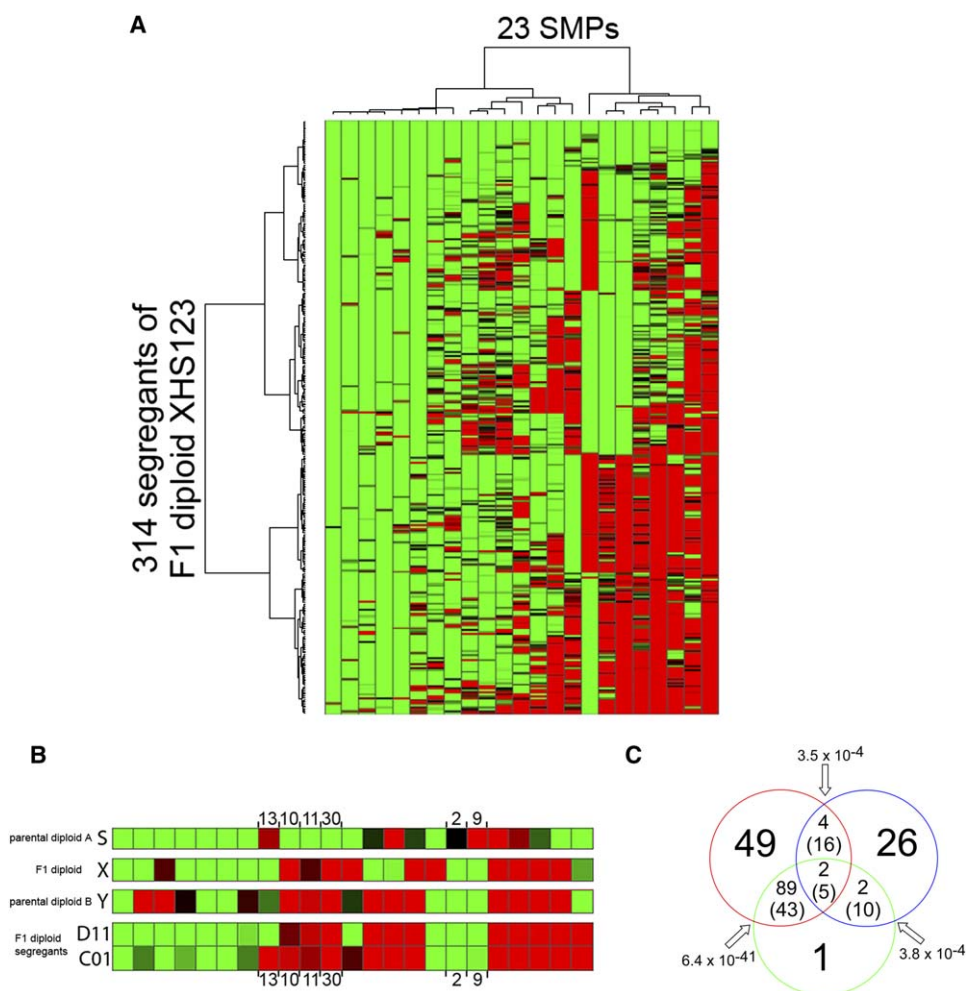
Figure 3. Dimensionality Reduction by 2D HAC Demonstrates Random and Independent Assortment of Genetic Determinants Underlying Resistance or Sensitivity to Each SMP

(A) 2D clustergram of a 314 × 23 matrix; each column is a small molecule; each row is a segregant; red indicates saturating growth, or resistance; green indicates no growth, or sensitivity.

(B) Small-molecule complex trait profiles of S1029 ("S"), XHS123 ("X"), YAG040 ("Y"), and two XHS123 segregants, D11 and C01, possess sensitivity profiles that are highly similar to that of YAG040. From left to right, identity of SMPs are: SMP17, SMP7, SMP48, SMP21, SMP49, SMP16, SMP45, SMP13, SMP10, SMP11, SMP30, SMP36, SMP3, SMP22, CSM-URA, G418, SMP2, SMP9, SMP50, SMP5, SMP33, SMP38, and SMP51.

(C) Venn diagram depicting phenotypic linkage and antilinkage. The large number in the red circle indicates how many segregants are resistant to 50 μg/ml flunarizine (SMP9), in the blue circle indicates how many segregants are resistant to 25 μg/ml FCCP (SMP21), and in the green circle indicates how many segregants are resistant to 25 μg/ml calcimycin (SMP2). The small numbers in the overlapping region correspond to the observed number of coresistant segregants, while the numbers in parentheses correspond to the expected number of coresistant segregants. The significance of overlaps (p value, hypergeometric distribution) between SMP9 resistance and SMP21 resistance (red and blue), SMP9 resistance and SMP2 resistance (red and green), and SMP21 resistance and SMP2 resistance (blue and green) are indicated with arrows.

genetic determinants that underlie resistance or sensitivity to each SMP). Several key observations affirm the latter. First, we observed unlinked segregation of resistance to flunarizine and to G418 (Figure 1C) in the 314-member library of segregants, as well as in tetrad dissections. Second, as shown in Figure 3A, red (resistant) and green (sensitive) slashes, which correspond to the growth of individual segregants in various SMPs, are generally randomly distributed in the clustergram that was generated by two-dimensional hierarchical agglomerative clustering (2D-HAC), a method of dimensionality reduction. The segregation of the URA3:: kanMX4 control Mendelian locus largely defines the overall structure of the clustergram.

In order to illustrate random segregation and independent assortment more clearly, we compared the resistance/sensitivity profiles of the parental and hybrids and several similar segregants. The parental and hybrid responses to nearly all of the 23 SMPs differed, as shown in Figure 3B and in Figure S1. Remarkably, however, there were instances where recombination preserved the parental and hybrid resistances and/or sensitivities, except at one or a few positions (Figure 3B). For example, one of the two segregants whose resistance/sensitivity profile is similar to that of YAG040, C01, inherited resistance to tunicamycin, an inhibitor of protein glycosylation [17], while the other, D11, did not (Figure 3B). This result is true for the majority of SMPs,
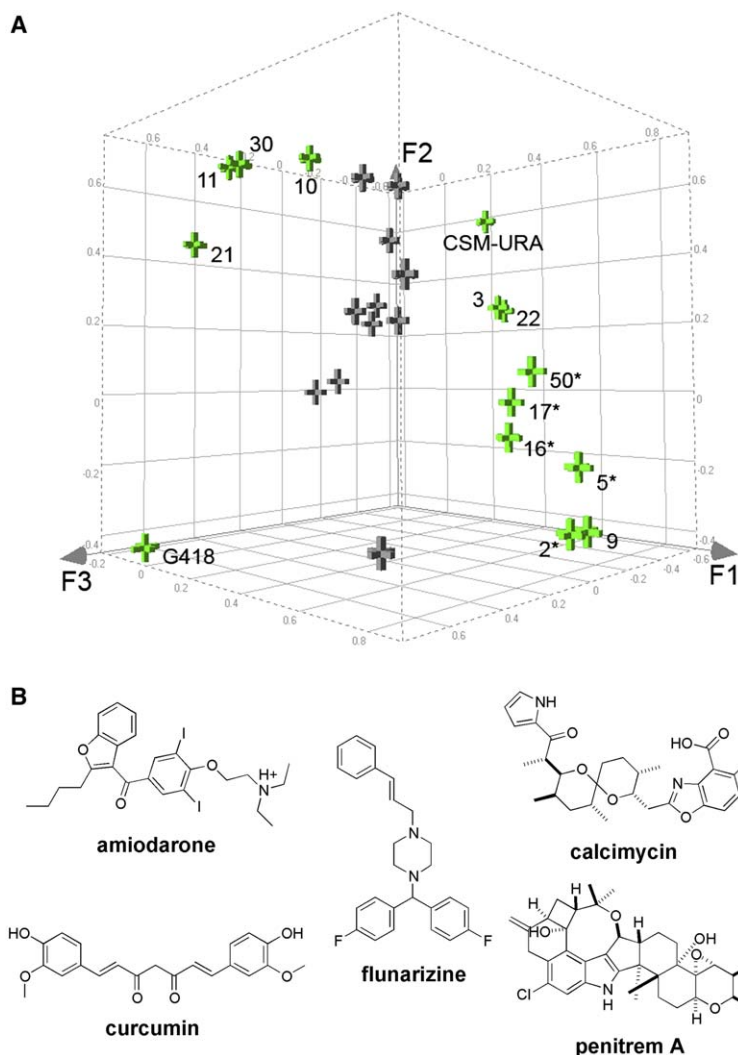
Figure 4. Principal Component Analysis Renders a 3D Chemical Space of SMPs that Illustrates the Notion of Functional Analogs

(A) 2D projection of a 3D PCA chemical space whose axes correspond to the first three principal components (F1, F2, and F3). Tacks represent SMPs; green tacks are labeled by corresponding SMP names; asterisked tacks represent SMPs that are modulators of Ca^{2+} homeostasis.

(B) Structures of a group of modulators of Ca^{2+} homeostasis: penitrem A (SMP50); amiodarone (SMP17); flunarizine (SMP9); curcumin (SMP5); calcimycin (SMP2).

suggesting that a unique set of genetic determinants selectively confers resistance to each SMP.

Next, we examined the SMPs for which the underlying genetic determinants of resistance or sensitivity appeared to be the same. We used principal component analysis (PCA), another method of dimensionality reduction, in order to render a three-dimensional (3D) "chemical space" of SMPs (Figure 4A). We observe clusters of SMPs that have been described previously as targeting the same proteins or pathways in cells ("functional analogs"); for comparison, G418 and CSM-URA, which are completely orthogonal to each other, reside in opposite corners of chemical space.

One cluster consists of flunarizine, amiodarone [18] (SMP17), calcimycin [19] (SMP2), curcumin [20] (SMP5), and penitrem A [21] (SMP50), all structurally dissimilar modulators of calcium ion homeostasis (Figure 4B). A second cluster consists of two known and two putative modulators of respiratory metabolism, respectively: menadione [22] (SMP30) and carbonyl cyanide 4-trifluoromethoxy-phenylhydrazone [23] (FCCP) (SMP21); and LY83583 [24] (SMP11) and 1,9-pyrazoloanthrone [25] (SMP10). A third cluster contains two structurally different antagonists of a master regulator

of Ca^{2+}-mediated signaling, calmodulin *CMD1*: chlorpromazine [26] and E6-berbamine [27]. Overall, our results suggest that this method also enables insights into mechanisms of small molecules, since small molecules with unknown mechanisms of action can be grouped together with those having known mechanisms.

We determined the degree of linkage between functional analogs on the basis of a probability test (p value, hypergeometric distribution) between pairs of traits. We observed significant (phenotypic) linkage between SMPs in each of the three aforementioned clusters of functional analogs. On the other hand, two blocs of resistance stand out as antilinked: dominant resistance to three compounds—FCCP (SMP21), LY83583 (SMP11), and 1,9-pyrazoloanthrone (SMP10)—that affect respiratory metabolism that may be encoded by YAG040-derived determinants; and recessive resistance to two compounds—calcimycin (SMP2) and flunarizine (SMP9)—that affect Ca^{2+} homeostasis that may be encoded by S288c-derived loci (Figure 3B). Antilinkage may occur when the same genetic determinant confers the opposite effect on two different SMPs. We are unaware of anything about Ca^{2+} homeostasis in the
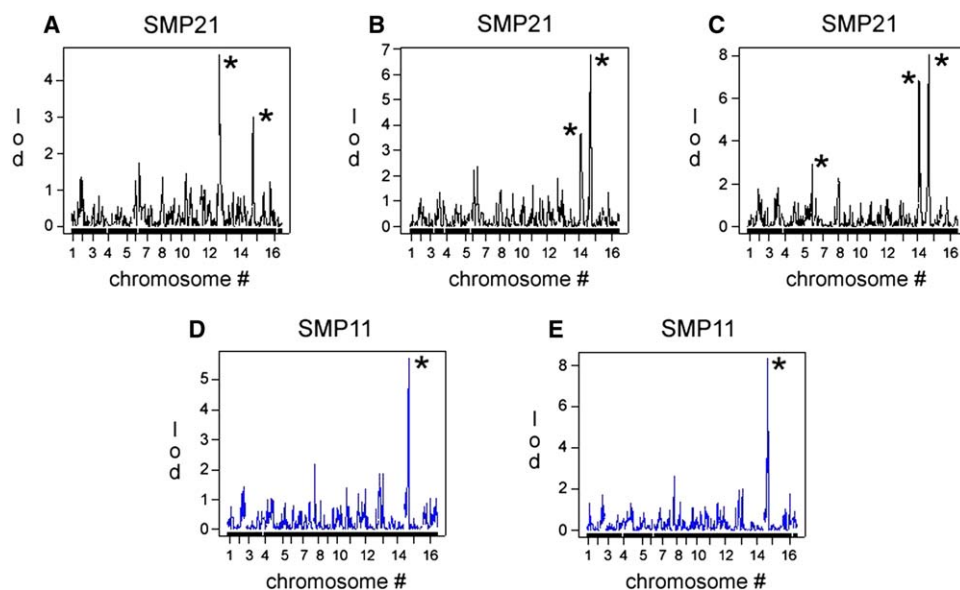
Figure 5. Genetic Mapping Confirms the Complex and Kinetic Nature of the Response to Small Molecules in a Population of 104 Naturally Recombinant Yeast Strains

LOD score is depicted on the y axis; the centers of yeast chromosomes (CHRI-XVI) are depicted as ticks on the x axis; asterisks denote linkage peaks.

(A) Linkage of chromosomal intervals on CHRXIII (peak at base pair 27,644) and CHRXV (peak at base pair 250,452) to the resistance to 5 μg/ml SMP21 at 40 hr postinoculation.

(B) Linkage of chromosomal intervals on CHRXIV (peak at base pair 476,445) and CHRXV (peak at base pair 250,452) to the resistance to 5 μg/ml SMP21 at 64 hr post inoculation.

(C) Linkage of chromosomal intervals on CHRVI (peak at base pair 183,351), CHRXIV (peak at base pair 472,845), and CHRXV (peak at base pair 250,452) to the resistance to 5 μg/ml SMP21 at 74 hr postinoculation.

(D) Linkage of a single chromosomal interval on CHRXV (peak at base pair 249,552) to the resistance to 6.7 μg/ml SMP11 at 40 hr postinoculation.

(E) Linkage of a single chromosomal interval on CHRXV (peak at base pair 250,452) to the resistance to 6.7 μg/ml SMP11 at 48 hr postinoculation.

YAG040 background that can explain its sensitivity, and vice versa, for S1029. However, S1029, as an S288c-derived strain, harbors a mutation in the gene *HAP1*, which results in constitutively low levels of cytochrome c [28], while YAG040 encodes the wild-type copy of *HAP1*. The sensitivity of S1029 to modulators of respiratory metabolism is consistent with it having a fragile respiratory apparatus.

A total of 34 segregants are resistant to FCCP (SMP21), 144 are resistant to flunarizine (SMP9), but only 4 (1%) are coresistant to both (p = 3.5 × 10⁻⁴; hypergeometric distribution) when 16 (5%) are expected by chance (Figure 3C). Moreover, dually resistant segregants treated simultaneously with both FCCP and flunarizine failed to grow even though they grew in the presence of each SMP alone, indicating that simultaneous small-molecule perturbation of Ca²⁺ homeostasis and respiratory processes results in synthetic lethality (Figure S5). Synthetic lethality between two SMPs may be the result of phenotypic antilinkage if a genetic determinant that confers resistance to flunarizine sensitizes yeast cells to FCCP, and vice versa. This codependence of Ca²⁺ homeostasis and respiratory processes is validated by extensive literature that documents the dependence of mitochondrial function on calcium [29], although no links have been drawn between these two functional processes by natural genetic variation in yeast.

We confirmed that the response to small molecules is indeed complex and kinetic, as well as the generality of our approach, by mapping the chromosomal regions that contain the genetic determinants underlying resistance to two SMPs in a cross between the S288c laboratory strain and a different natural isolate, RM11. Specifically, we tested for linkage over several time points between resistance to two functional analogs that affect respiratory processes, LY83583 (SMP11) and FCCP (SMP21), and genetic markers in 104 previously genotyped segregants derived from a cross between BY4716 (isogenic to S288c) and RM11-1a, an agricultural isolate [30, 31].

Linkage was tested at three time points in the case of SMP21—early, intermediate, and late—and two time points in the case of SMP11—early and intermediate. We report the results in terms of logarithm of odds (LOD) scores. We assessed significance via 100 permutations for each compound and time point, and considered LOD scores higher than any seen in the 100 permutations for that compound and time point as highly significant (genome-wide empirical p = 0.01), and those LOD scores exceeded in 5 or fewer of the 100 permutations as significant (genome-wide empirical p = 0.05). LOD scores above 3 but not significant by these criteria were considered suggestive of linkage.

At the early time point, we observed a highly significant linkage of SMP21 resistance to a quantitative trait

locus (QTL) spanning less than 1 kb on the left arm of chromosome 13 (LOD score = 4.7) and a weaker, suggestive linkage to a QTL spanning around 30 kb on the left arm of chromosome 15 (LOD score = 3.0). The weak QTL on chromosome 15 links more strongly at later time points, with highly significant LOD scores of 6.8 and 8.1 at the intermediate and late time points, respectively. At the intermediate time point, we observed another suggestive linkage (LOD score = 3.6) to a QTL spanning approximately 50 kb on the left arm of chromosome 14, and this linkage became highly significant at the late time point (LOD score = 6.9). At the late time point, we observed another suggestive linkage to a QTL spanning 25 kb on the right arm of chromosome 6 (Figures 5A–5C). In total, we observed three highly significant and one suggestive QTL linked to the response to SMP21. The QTL on the left arm of chromosome 15 that links to SMP21 also links to resistance to SMP11 as a 10 kb interval, with highly significant LOD scores of 5.7 and 8.3 at the early and intermediate time points, respectively (Figures 5D and 5E), thus providing direct genetic evidence that SMP11 and SMP21 are functional analogs, and further increasing our confidence in the linkages. Interestingly, none of the QTLs contains genes known to be involved in the response to xenobiotics. Furthermore, as our linkage analysis removes QTLs that link to growth in the DMSO control condition, we rule out the role of intrinsic differences in growth rates among the 104 segregants as a contributing factor in the response to either compound.

Significance

This work illustrates a general, scalable, low-cost, chemical-genetic method for revealing complex traits in budding yeast. Cumulatively, the SMPs we used perturb a wide swath of cellular processes, but, individually, the genes with which they interact are distinct, except in the case of functional analogs whose common reported mechanisms of action we validated. The extensive characterization of natural genetic variation with small molecules complements the use of de novo or artificial mutations in a fixed genetic background, since most naturally occurring mutations are not neat excisions of open reading frames. The systematic combination of natural variants of yeast and small molecules that modulate evolutionarily conserved cellular processes may have several applications: (1) as a small-molecule classifier—used to identify mechanisms of action of small molecules; (2) the classification and characterization of genetic traits (Mendelian versus complex); and (3) the systematic mapping of complex traits in a single organism ("phenomics") [32].

Experimental Procedures

Yeast Strains
Parental diploid strains S1029, an S288c derivative (*MAT*a/*MAT*-alpha gal2/gal2 hoD::natMX4/hoD::natMX4), and YAG040 (HO/hoD::hphMX4 *MAT*a/*MAT*alpha), along with F1 hybrid strain XHS123 (URA3/ura3D::kanMX4), were generous gifts from John H. McCusker, Duke University, Durham, NC. A total of 104 genotyped segregants from the BY4716/RM11-1a cross were previously described [30]. The kanMX resistance cassette encodes a phospho-

transferase that confers resistance to the aminoglycoside G418 (geneticin) while replacing the S288c-derived copy of URA3, a gene involved in uracil biosynthesis; the hphMX resistance cassette encodes a phosphotransferase that confers resistance to the aminoglycosin hygromycin B while replacing one copy of the HO gene, the endonuclease responsible for mating-type switching. XHS123 is HO/ho, which means that we expect approximately 50% of segregants to be haploid (ho) and 50% to be diploid (HO) as a result of self-diploidization. We find no significant effect of ploidy on growth, except a subtle growth advantage to homozygous diploid recombinants that is undetectable by the 48 hr time point. For added stringency, we considered 375 *MAT*a haploid segregants in our estimation of polygenic degree on the basis of sensitivity to the mating pheromone α factor.

Natural Recombinant Yeast Library Generation
Culturing and sporulation of yeast as well as media formulation was done as previously described [33]. XHS123 segregants were derived as random spores (not by tetrad dissection). They were manually arrayed from dabs of single colonies grown on agar plates into individual wells of 384-well plates containing rich media to make strain stock plates. NUNC 384-well, clear-bottom, untreated, sterile plates (VWR, no. 62409-604) containing rich media and either vehicle solvent (dimethyl sulfoxide [DMSO]) or a given SMP were inoculated with yeast from strain stock plates using sterile polypropylene 384-pin replicators (Genetix, no. X5050). Inoculated plates were grown without agitation on the benchtop at ambient temperature conditions for 48–72 hr, and then vortexed on a standard tabletop vortexer (VWR) for 10–30 s prior to measurement in a SpectraMax plate reader (Molecular Devices) set to 600 nm emission. The growth of each XHS123 segregant in rich media containing a given SMP was compared to its growth in media containing DMSO. We used the reciprocal segregation of the kanMX and URA3 markers as a positive indicator of recombination, and discarded products of sporulation that were neither G418^{SEN}/URA$^+$ nor G418^{RES}/URA$^-$. We arrived at 314 segregants in the smaller library because at least 314 of 380 (83%) products of sporulation passed the recombination test. We arrived at 1932 segregants (375 of which are *MAT*a, as assessed by sensitivity to the mating pheromone α factor) in the larger library because at least 1932 of 2944 (66%) products of sporulation passed the recombination test. The discarded products of sporulation are either extremely slow-growing segregants or contaminating diploids (G418^{RES}/URA$^+$). Cut-offs of resistance and sensitivity were visually assessed with the rank-ordered distributions of the segregants grown in the presence of each SMP.

SMPs
SMPs were individually purchased as powder stocks from various vendors in either 10 mg or smaller quantities, and then resuspended in DMSO in glass vials as stock solutions: calcimycin (Biomol, no. CA-100); E6-berbamine (Biomol, no. CA-302); curcumin (Biomol, no. EI-135); doxorubicin (Biomol, no. GR-319); flunarizine (Biomol, no. CA-225); 1,9-pyrazoloanthrone (EMD Biosciences, no. 420119); LY83583 (Biomol, no. CN-200); tunicamycin (Biomol, no. CC-104), anisomycin (Biomol, no. ST-102); amiodarone (Biomol, AC-105); FCCP (Sigma-Aldrich, no. C2920); chlorpromazine (EMD Biosciences, no. 215921); menadione (Sigma-Aldrich, no. M5625); pimozide (Tocris, no. 0937); diphenyleneiodonium (Sigma-Aldrich, no. D2926); spermine NONOate (EMD Biosciences, no. 567703); rapamycin (EMD Biosciences, no. 553210); manumycin (Biomol, no. G-236); mastoparan (EMD Biosciences, no. 444898); penitrem A (Biomol, no. KC-157); wortmannin (EMD Biosciences, no. 681675). See the NCI-sponsored public database ChemBank (http://chembank.med.harvard.edu) for complete structural annotations and mechanisms of action.

Computational Dimensionality Reduction
Duplicate measurements were averaged and arranged in a matrix, S, as shown in Figure 1A, consisting of an ordered array of rows and columns. Each row (x_i, where i = 1 to m) corresponds to growth of a particular segregant across the set of SMPs; each column (y_j, where j = 1 to n) corresponds to a particular SMP. Accordingly, an element (x_m, y_n) of S encodes information about segregant m for phenotypic descriptor n. 2D-HAC and p values based on the

hypergeometric distribution were computed using XLSTAT-Pro7.1 (Addingsoft) in Microsoft Excel; PCA and data visualization was performed by Spotfire DecisionSite v.7.0 (Spotfire, Inc.).

Linkage Analysis

All linkage analysis was performed using the R/Qtl software package [34], and significance was assessed via permutations. The analysis was done using a set of 104 segregants and 2972 markers. Phenotypes and genotypes were arranged into the proper csv file format for direct input into R/Qtl. Phenotypes (responses to small molecules) were scanned under the default (normal) single QTL model using the standard EM algorithm. All control (DMSO-treated) phenotypes were used as additive covariates in order to eliminate their effect on linkage.

Supplemental Data

Supplemental Data, including a table and figures, are available online at http://www.chembiol.com/cgi/content/full/13/3/319/DC1/.

References

1. Forsburg, S.L. (2001). The art and design of genetic screens: yeast. Nat. Rev. Genet. 2, 659–668.

2. Tong, A.H., and Boone, C. (2005). Synthetic genetic array analysis Saccharomyces cerevisiae. Methods Mol. Biol. 313, 171–192.

3. Abiola, O., Angel, J.M., Avner, P., Bachmanov, A.A., Belknap, J.K., Bennett, B., Blankenhorn, E.P., Blizard, D.A., Bolivar, V., Brockmann, G.A., et al. (2003). The nature and identification of quantitative trait loci: a community's view. Nat. Rev. Genet. 4, 911–916.

4. Anholt, R.R.H., and Mackay, T.F.C. (2004). Quantitative genetic analyses of complex behaviours in Drosophila. Nat. Rev. Genet. 5, 838–849.

5. Arnold, P.D., Zai, G., and Richter, M.A. (2004). Genetics of anxiety disorders. Curr. Psychiatry Rep. 6, 243–254.

6. Parsons, A.B., Brost, R.L., Ding, H., Li, Z., Zhang, C., Sheikh, B., Brown, G.W., Kane, P.M., Hughes, T.R., and Boone, C. (2004). Integration of chemical-genetic and genetic interaction data links bioactive compounds to cellular target pathways. Nat. Biotechnol. 22, 62–69.

7. Giaever, G., Flaherty, P., Kumm, J., Proctor, M., Nislow, C., Jaramillo, D.F., Chu, A.M., Jordan, M.I., Arkin, A.P., and Davis, R.W. (2004). Chemogenomic profiling: identifying the functional interactions of small molecules in yeast. Proc. Natl. Acad. Sci. USA 101, 793–798.

8. Beadle, G.W., and Tatum, E.L. (1941). Genetic control of biochemical reactions in Neurospora. Proc. Natl. Acad. Sci. USA 27, 499–506.

9. Brem, R.B., Yvert, G., Clinton, R., and Kruglyak, L. (2002). Genetic dissection of transcriptional regulation in budding yeast. Science 296, 752–755.

10. Yvert, G., Brem, R.B., Whittle, J., Akey, J.M., Foss, E., Smith, E.N., Mackelprang, R., and Kruglyak, L. (2003). Trans-acting regulatory variation in Saccharomyces cerevisiae and the role of transcription factors. Nat. Genet. 35, 57–64.

11. Marullo, P., Bely, M., Masneuf-Pomarede, I., Aigle, M., and Dubourdieu, D. (2004). Inheritable nature of enological quantitative traits is demonstrated by meiotic segregation of industrial wine yeast strains. FEM. Yeast Res. 4, 711–719.

12. Deutschbauer, A.M., and Davis, R.W. (2005). Quantitative trait loci mapped to single-nucleotide resolution in yeast. Nat. Genet. 37, 1333–1340.

13. Steinmetz, L.M., Sinha, H., Richards, D.R., Spiegelman, J.I., Oefner, P.J., McCusker, J.H., and Davis, R.W. (2002). Dissecting the architecture of a quantitative trait locus in yeast. Nature 416, 326–330.

14. Gu, Z., David, L., Petrov, D., Jones, T., Davis, R.W., and Steinmetz, L.M. (2005). Elevated evolutionary rates in the laboratory strain of Saccharomyces cerevisiae. Proc. Natl. Acad. Sci. USA 102, 1092–1097.

15. Amery, W.K. (1983). Flunarizine, a calcium channel blocker: a new prophylactic drug in migraine. Headache 23, 70–74.

16. Lum, P.Y., Armour, C.D., Stepaniants, S.B., Cavet, G., Wolf, M.K., Butler, J.S., Hinshaw, J.C., Garnier, P., Prestwich, G.D., Leonardson, A., et al. (2004). Discovering modes of action for therapeutic compounds using a genome-wide screen of yeast heterozygotes. Cell 116, 121–137.

17. Elbein, A.D. (1984). Inhibitors of the biosynthesis and processing of N-linked oligosaccharides. CRC Crit. Rev. Biochem. 16, 21–49.

18. Pozniakovsky, A.I., Knorre, D.A., Markova, O.V., Hyman, A.A., Skulachev, V.P., and Severin, F.F. (2005). Role of mitochondria in the pheromone- and amiodarone-induced programmed death of yeast. J. Cell Biol. 168, 257–269.

19. Gruetter, C.A., Lemke, S.M., Valentovic, M.A., and Szarek, J.L. (1994). Evidence that histamine is involved as a mediator of endothelium-dependent contraction induced by A23187 in bovine intrapulmonary vein. Eur. J. Pharmacol. 257, 275–283.

20. Logan-Smith, M.J., Lockyer, P.J., East, J.M., and Lee, A.G. (2001). Curcumin, a molecule that inhibits the Ca^{2+}-ATPase of sarcoplasmic reticulum but increases the rate of accumulation of Ca^{2+}. J. Biol. Chem. 276, 46905–46911.

21. Knaus, H.G., McManus, O.B., Lee, S.H., Schmalhofer, W.A., Garcia-Calvo, M., Helms, L.M., Sanchez, M., Giangiacomo, K., Reuben, J.P., Smith, A.B., III, et al. (1994). Tremorgenic indole alkaloids potently inhibit smooth muscle high-conductance calcium-activated potassium channels. Biochemistry 33, 5819–5828.

22. Shapira, M., Segal, E., and Botstein, D. (2004). Disruption of yeast forkhead-associated cell cycle transcription by oxidative stress. Mol. Biol. Cell 15, 5659–5669.

23. Heytler, P.G., and Prichard, W.W. (1962). A new class of uncoupling agents—carbonyl cyanide phenylhydrazones. Biochem. Biophys. Res. Commun. 7, 272–275.

24. Lodygin, D., Menssen, A., and Hermeking, H. (2002). Induction of the Cdk inhibitor p21 by LY83583 inhibits tumor cell proliferation in a p53-independent manner. J. Clin. Invest. 110, 1717–1727.

25. Shin, M., Yan, C., and Boyd, D. (2002). An inhibitor of c-jun aminoterminal kinase (SP600125) represses c-Jun activation, DNA-binding and PMA-inducible 92-kDa type IV collagenase expression. Biochim. Biophys. Acta 1589, 311–316.

26. Wiley, J.S., and McCulloch, K.E. (1982). Calcium ions, drug action and the red cell membrane. Pharmacol. Ther. 18, 271–292.

27. Zhu, H.J., and Liu, G.Q. (2003). Effect of E6, a novel calmodulin inhibitor, on activity of P-glycoprotein in purified primary cultured rat brain microvessel endothelial cells. Acta Pharmacol. Sin. 24, 1143–1149.

28. Gaisne, M., Becam, A.M., Verdiere, J., and Herbert, C.J. (1999). A 'natural' mutation in Saccharomyces cerevisiae strains derived from S288c affects the complex regulatory gene HAP1 (CYP1). Curr. Genet. 36, 195–200.

29. Gunter, T.E., Yule, D.I., Gunter, K.K., Eliseev, R.A., and Salter, J.D. (2004). Calcium and mitochondria. FEBS Lett. 567, 96–102.

30. Brem, R.B., and Kruglyak, L. (2005). The landscape of genetic complexity across 5,700 gene expression traits in yeast. Proc. Natl. Acad. Sci. USA 102, 1572–1577.

31. Mortimer, R.K., Romano, P., Suzzi, G., and Polsinelli, M. (1994). Genome renewal: a new phenomenon revealed from a genetic

study of 43 strains of *Saccharomyces cerevisiae* derived from natural fermentation of grape musts. Yeast *10*, 1543–1552.

32. Freimer, N., and Sabatti, C. (2003). The human phenome project. Nat. Genet. *34*, 15–21.

33. Ausubel, F.M., Brent, R., Kingston, R.E., Moore, D.D., Seidman, J.G., Smith, J.A., and Struhl, K., eds. (1996). Current Protocols in Molecular Biology, Volume 2 (New York: John Wiley and Sons).

34. Broman, K.W., Wu, H., Sen, S., and Churchill, G.A. (2003). R/qtl: QTL mapping in experimental crosses. Bioinformatics *19*, 889–890.